

Voltage control of ferromagnetic resonance and spin waves

Xinger Zhao(赵星儿), Zhongqiang Hu(胡忠强), Qu Yang(杨曲), Bin Peng(彭斌), Ziyao Zhou(周子尧), Ming Liu(刘明)

Citation: Chin. Phys. B . 2018, 27(9): 097505. **doi:** 10.1088/1674-1056/27/9/097505

Journal homepage: http://cpb.iphy.ac.cn; http://iopscience.iop.org/cpb

What follows is a list of articles you may be interested in

Voltage control of magnetization switching and dynamics

Hong-Yu Wen(文宏玉), Jian-Bai Xia(夏建白)

Chin. Phys. B . 2018, 27(6): 067502. **doi:** 10.1088/1674-1056/27/6/067502

Shape-manipulated spin-wave eigenmodes of magnetic nanoelements

Zhang Guang-Fu, Li Zhi-Xiong, Wang Xi-Guang, Nie Yao-Zhuang, Guo Guang-Hua

Chin. Phys. B . 2015, 24(9): 097503. **doi:** 10.1088/1674-1056/24/9/097503

Dynamics of magnetization in ferromagnet with spin-transfer torque

Li Zai-Dong, He Peng-Bin, Liu Wu-Ming

Chin. Phys. B . 2014, 23(11): 117502. **doi:** 10.1088/1674-1056/23/11/117502

Ferromagnetic resonance frequency shift model of laminated magnetoelectric structure tuned by electric field

Zhou Hao-Miao, Chen Qing, Deng Juan-Hu

Chin. Phys. B . 2014, 23(4): 047502. **doi:** 10.1088/1674-1056/23/4/047502

Flexible tuning microwave permeability spectrum in [ferromagnet/antiferromagnet]$_n$ exchange-biasedmultilayer stack structure

Jin Li-Chuan, Zhang Huai-Wu, Tang Xiao-Li, Bai Fei-Ming, Zhong Zhi-Yong

Chin. Phys. B . 2013, 22(4): 047502. **doi:** 10.1088/1674-1056/22/4/047502

TOPICAL REVIEW — Spin manipulation in solids

Voltage control of ferromagnetic resonance and spin waves*

Xinger Zhao(赵星儿), Zhongqiang Hu(胡忠强)†, Qu Yang(杨曲),
Bin Peng(彭斌), Ziyao Zhou(周子尧)‡, and Ming Liu(刘明)

Electronic Materials Research Laboratory, Key Laboratory of the Ministry of Education & International Center for Dielectric Research, School of Electronic and Information Engineering, Xi'an Jiaotong University, Xi'an 710049, *China*

(Received 30 April 2018; revised manuscript received 29 May 2018; published online 28 August 2018)

The voltage control of magnetism has attracted intensive attention owing to the abundant physical phenomena associated with magnetoelectric coupling. More importantly, the techniques to electrically manipulate spin dynamics, such as magnetic anisotropy and ferromagnetic resonance, are of great significance because of their potential applications in high-density memory devices, microwave signal processors, and magnetic sensors. Recently, voltage control of spin waves has also been demonstrated in several multiferroic heterostructures. This development provides new platforms for energy-efficient, tunable magnonic devices. In this review, we focus on the most recent advances in voltage control of ferromagnetic resonance and spin waves in magnetoelectric materials and discuss the physical mechanisms and prospects for practical device applications.

Keywords: voltage control, ferromagnetic resonance, spin wave, magnetoelectric coupling

PACS: 75.85.+t, 76.50.+g, 75.30.Ds **DOI:** 10.1088/1674-1056/27/9/097505

1. Introduction

Numerous physical phenomena related to ferromagnetic resonance (FMR) and spin wave resonance (SWR) promote investigations of not only fundamental properties, but also practical applications.[1,2] Wave-based computing with an additional degree of freedom provided by the utilization of the phase of spin waves could reduce the amount of space that each memory cell requires.[3,4] The feature with a wide frequency range (GHz to THz) exhibits distinct advantages in communication systems and radars.[2,5,6] Therefore, wave-based devices are of great investigative significance due in part to their potential to considerably reduce heat dissipation because of the absence of electron migration.[7]

A spin wave originates from the disturbance of local magnetic ordering propagation in magnetic materials, and the magnon is the quanta of a spin wave.[8] The uniform FMR mode, which is the spatially uniform precession of magnetization over the whole sample, is the lowest energy magnon with the wave vector $k = 0$.[9] Two theoretical models have been proposed to interpret phenomena related to spin waves, the volume inhomogeneity model and the surface inhomogeneity model. These models each have different forms of surface spin pinning conditions.[10] The pinning condition of the latter model is the solution of a Hamiltonian calculated by Puszkarski, which can be depicted by a surface parameter A given by[11,12]

$$A = 1 - (g\mu_{\mathrm{B}}/2S_zJ)\,(\boldsymbol{K}_{\mathrm{s}}\cdot\boldsymbol{\gamma}), \tag{1}$$

where g is the spectroscopic-splitting factor, μ_{B} is the Bohr magneton, S is the spin, z is the atomic number of the nearest neighbor, J is the Heisenberg interaction constant, $\boldsymbol{K}_{\mathrm{s}}$ is the surface anisotropy field under surface spin, and $\boldsymbol{\gamma}$ is the unit vector whose direction is parallel to the direction of the magnetization. Under the symmetric boundary condition, the state with $A = 1$ implies the uniform precession mode, i.e., FMR. Correspondingly, the state with $A < 1$ indicates that the body spin wave is excited and that with $A > 1$ implies that both the body spin and surface spin waves can be motivated.

Even though it is more common to modulate magnetism by means of a magnetic field or a spin-current injection,[13–16] the related Joule heat dissipation cannot be ignored for certain applications, and especially in integrated circuits and systems. Consequently, it is of great importance to investigate other driving modes to implement the desired functionality. The modulation of magnetic properties including magnetic anisotropy, SWR, and FMR, etc. via voltage only involves the charge/discharge process of a capacitor in principle.[17] Remarkably, voltage control of magnetic anisotropy has resulted in many significant research results and promoted the exploration of voltage-controlled logic devices.[15,18–21] Currently most microwave devices are based on ferrites rather than mag-

*Project supported by the National Natural Science Foundation of China (Grant No. 51602244), the National 111 Project of China (Grant No. B14040), and the Fundamental Research Funds for the Central Universities, China (Grant No. xjj2018207).

†Corresponding author. E-mail: zhongqianghu@xjtu.edu.cn

‡Corresponding author. E-mail: ziyaozhou@xjtu.edu.cn

© 2018 Chinese Physical Society and IOP Publishing Ltd

netic metallic and alloy systems because the resistances of ferromagnetic metals and alloys are low and result in large eddy current losses at high frequency. However, ferromagnetic metals and alloys can be easily prepared on any substrates at room temperature, which also have high magnetorestriction leading to large tunability in strain-mediated magnetoelectric coupling, as has been highlighted in many reports.[15–19] Therefore, *in situ* observation of the FMR shift in ferromagnetic metals and alloys is a powerful tool for research involving voltage tuning of magnetism. This technique has potential applications in energy-efficient electronic devices, including magnetoelectric random access memory, magnetic field sensors, and tunable radio frequency (RF)/microwave devices. In this review, we focus on the most recent advances in voltage control of ferromagnetic resonance and spin waves in magnetoelectric materials, and discuss the physical mechanisms and prospects for practical device applications.

2. Voltage tuning of ferromagnetic resonance

Several mechanisms have been proposed for voltage control of magnetism including strain regulation,[22–24] charge modulation,[25] exchange coupling,[26] electrochemical effect,[27] and orbital reconstruction.[28] Cooperation and competition exist among those mechanisms, depending on the characteristic thickness of the magnetic films.[29] Specifically, charge modulation and orbital reconstruction modulation may play a leading role in film with thicknesses on the order of several nanometers, exchange coupling modification and electrochemistry modification dominate over the range of dozens of nanometers, and the strain/stress effect is dominant in relatively thicker films.[29–31] FMR absorption is an interesting resonance phenomenon which occurs when a magnetic field and a microwave field are applied to a ferromagnetic specimen simultaneously, and the resonance condition is satisfied.[9] Numerous research achievements have been reported on voltage tuning of FMR involving various geometries and materials.[9,32–36] Voltage control of magnetism may facilitate wide FMR modification in an energy efficient way for application in voltage-tunable spintronic devices.[37]

2.1. Voltage control of FMR via strain/stress

In a large number of investigations, strain/stress-mediated effects have become a desirable approach to regulate FMR.[38–41] In multiferroic heterostructures, the voltage applied across the thickness direction of piezoelectric/ferroelectric substrates induces the deformation of the piezoelectric/ferroelectric phase, which can be transmitted to the magnetic phase via magnetoelectric (ME) coupling. Thus, the purpose of adjusting the FMR by voltage is realized.

By using the Kittel equation, the FMR frequency can be derived as[42]

$$\text{in-plane:}\quad f=\gamma\sqrt{(H_{\rm r}+H_{\rm eff})\,(H_{\rm r}+H_{\rm k}+H_{\rm eff}+4\pi M_{\rm s})}, \quad (2)$$

$$\text{out-of-plane:}\quad f=\gamma\,(H_{\rm r}+H_{\rm k}+H_{\rm eff}-4\pi M_{\rm s})\,, \quad (3)$$

where f is the FMR frequency, $H_{\rm r}$ is the FMR field, $H_{\rm eff}$ is the effective field induced by the voltage, $H_{\rm k}$ is the anisotropy field, and $M_{\rm s}$ is the saturation magnetization. It is evident from formulas (2) and (3) that the regulation of the FMR field and frequency can be accomplished by tuning $H_{\rm eff}$.[38,43]

2.1.1. Strain/stress modulation for materials with in-plane easy axis

From the perspective of microwave application, it is important to realize giant voltage modification of both the FMR frequency and the FMR field at room temperature. According to the intrinsic mechanism of the strain/stress-mediated ME coupling, a common method involves the utilization of materials with high magnetostriction values and high piezoelectric coefficients. Liu *et al.* achieved a large FMR tunability of 860 Oe with a corresponding linewidth of 330–380 Oe in Fe_3O_4/lead zinc niobate-lead titanate (PZN-PT) multiferroic heterostructures.[38] In addition, Liu *et al.* further demonstrated a remarkable FMR field variation of 3500 Oe with a large FMR linewidth of 1200 Oe in specially selected Terfenol-D/PZN-PT bilayer heterostructures.[44]

Nevertheless, the FMR measurements were often accompanied by a large FMR linewidth from the magnetic phase, which limits the practical application.[35,45] In order to reduce the FMR linewidth while maintaining giant electrical modulation, Liu *et al.* reported on a novel amorphous FeGaB film as a magnetic layer that retained strong absorption over a small linewidth of approximatively 50 Oe,[22] while preserving PZN-PT(011) as the piezoelectric substrate.[46] The 50-nm-thick FeGaB film was deposited onto PZN-PT(011) substrates utilizing co-sputtering of $Fe_{80}Ga_{20}$ and B targets. When a voltage was applied perpendicular to the piezoelectric substrate, the substrate experienced tensile stress along $[01\bar{1}]$ and compressive stress along [100] because of the opposite sign of the in-plane piezoelectric coefficients. The biaxial stress induced voltage tuning of the FMR in both the field- and frequency-sweeping modes, as shown in Fig. 1. At a fixed frequency of 11.3 GHz, the electric fields of $\pm$6 kV/cm induced an FMR field tunability of 1200 Oe, corresponding to a large ME coefficient of 100 Oe cm/ kV. If the magnetic field was set at 1518 Oe, the tunable range of the FMR frequency could be as high as 5.3 GHz. More importantly, a novel technological approach with dual E- and H-modulation of the FMR was introduced. The application of this method resulted in a tunable range of the FMR frequency up to 13.1 GHz.

Nevertheless, high eddy current losses in magnetic metals and alloys at a high frequency significantly limit the performance of microwave devices. This issue is noteworthy and cannot be neglected. A few investigations attempted to utilize magnetic metal or alloy/insulator multilayer films as microwave materials. In such cases, an inserted insulator was used to divide the magnetic metal or alloy layer into multiple thinner layers to reduce the eddy current loss.[47] Yang *et al.* reported on a single bandstop filter prototype based on FeGaB/Al_2O_3 multilayers with a tunability of over 55% and an insertion loss of a minimum of 0.5 dB.[48] Moreover, Gao *et al.* also prepared integrated GHz magnetic inductors with solenoid structures using FeGaB/Al_2O_3 multilayer films, for which the peak quality factor was close to 20.[49]

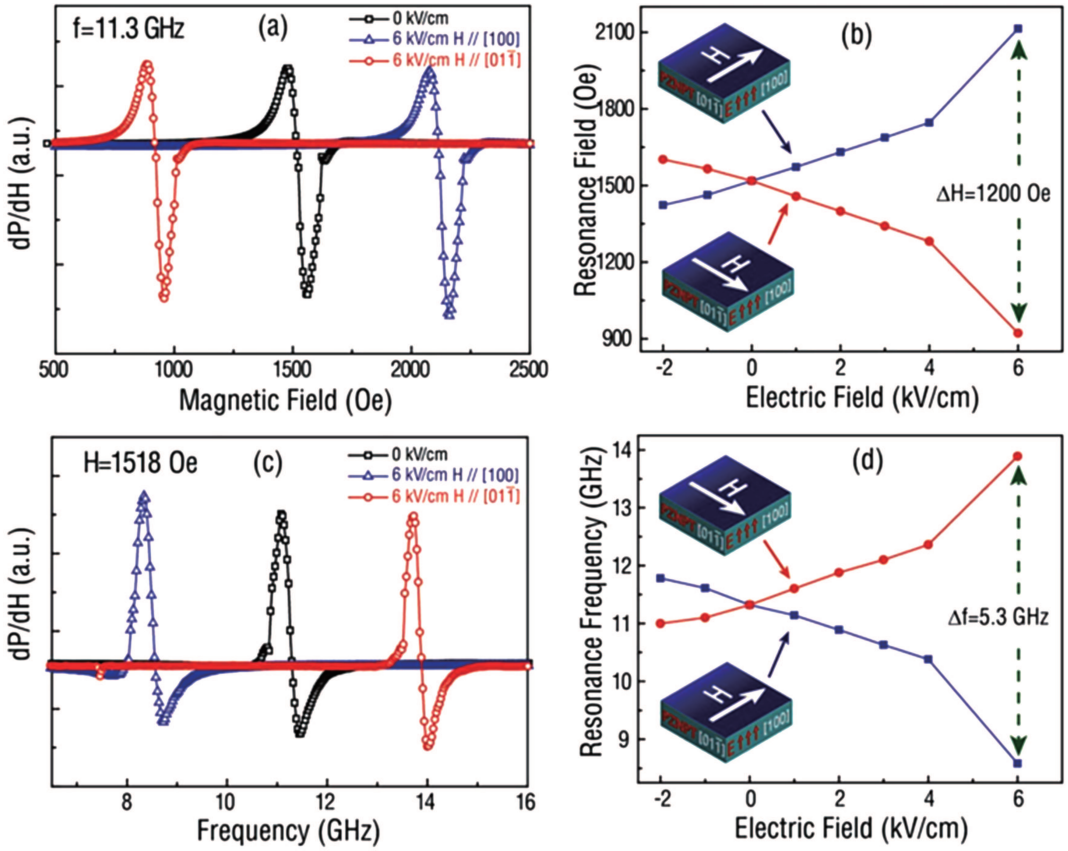


Fig. 1. (color online) Voltage control of FMR in (a), (b) field-sweeping and (c), (d) frequency-sweeping modes with a large tunability of 1200 Oe and 5.3 GHz, respectively.[46]

From an application point-of-view, single crystal piezoelectric materials cannot be readily integrated onto universal silicon substrates. This issue has limited their development. To address this problem, Gao *et al.* proposed a method to make the piezoelectric slab compatible with silicon-based techniques using deep reactive-ion etching (DRIE) to dislodge the silicon from the silicon-on-insulator (SOI) substrates after the deposition of the FeCoSiB film.[50] The FeCoSiB (100 nm)/Si (10 μm)/SiO_2 (50 nm) multilayer obtained by this method was epoxy bonded to a PMN-PT(011) substrate. FeCoSiB/PMN-PT(011) was also prepared under the same conditions as the object of reference. Figure 2 shows the voltage tuning of the FMR fields in both structures. For FeCoSiB/PMN-PT, the maximum modulation was 180 Oe with a linewidth in excess of 283 Oe. In contrast, the FeCoSiB/Si/SiO_2/PMN-PT exhibited approximately the same maximum tunability of 175 Oe with a much narrower linewidth of approximately 40 Oe. In addition, spin wave modes were observed at the lower field sides of the main peak in Fig. 2(c). Consequently, the proposed strategy was demonstrated to be effective in decreasing the substrate clamping effect and reducing the linewidth.

2.1.2. Strain/stress modulation for materials with out-of-plane easy axis

Materials exhibiting perpendicular magnetic anisotropy (PMA) have received increasing attention because of their potential to enhance thermal stability and ultrahigh storage density, which provides a feasible way to produce high-density memory devices.[51] Moreover, voltage control of PMA could further decrease thermal dissipation and thus suppress energy consumption. The variations via strain/stress in hysteresis loop, magnetic anisotropy energy, and FMR performance have been investigated for materials possessing PMA.[52–56]

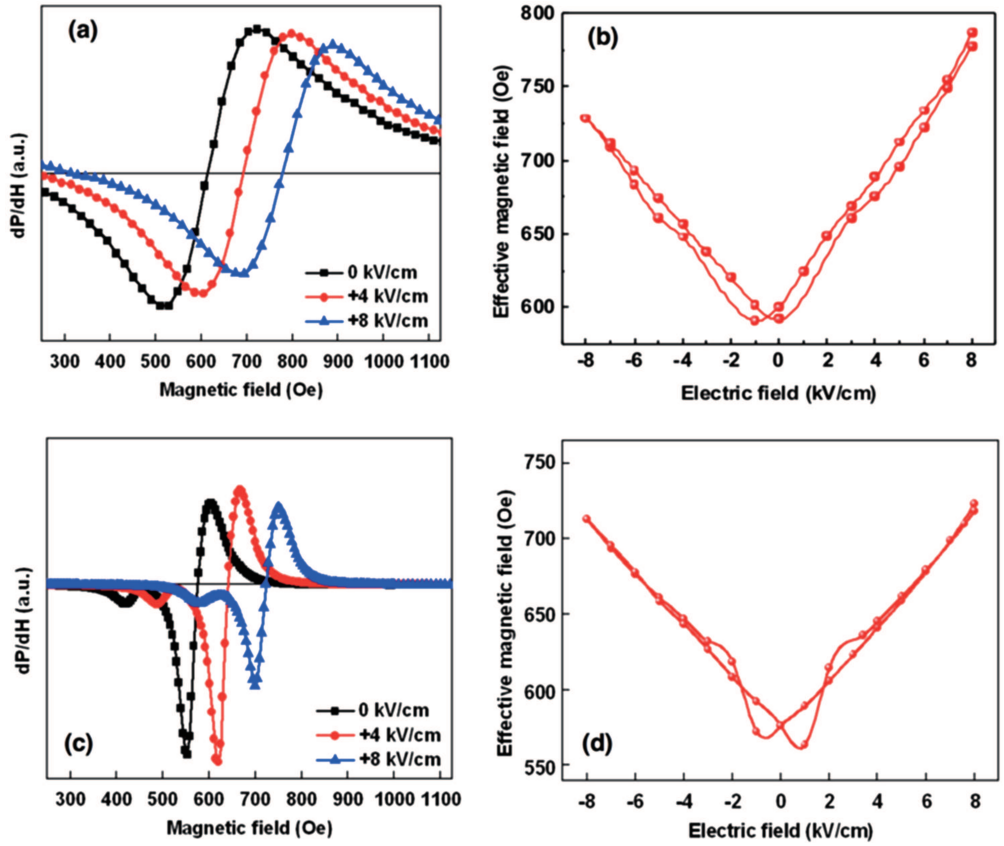


Fig. 2. (color online) (a), (c) FMR spectra and (b), (d) voltage dependence of FMR fields of the FeCoSiB/PMN-PT multiferroic heterostructures and FeCoSiB/Si/SiO_2/PMN-PT laminates at various electric fields, respectively. The external magnetic fields were all along the [01$\bar{1}$] direction of PMN-PT.[50]

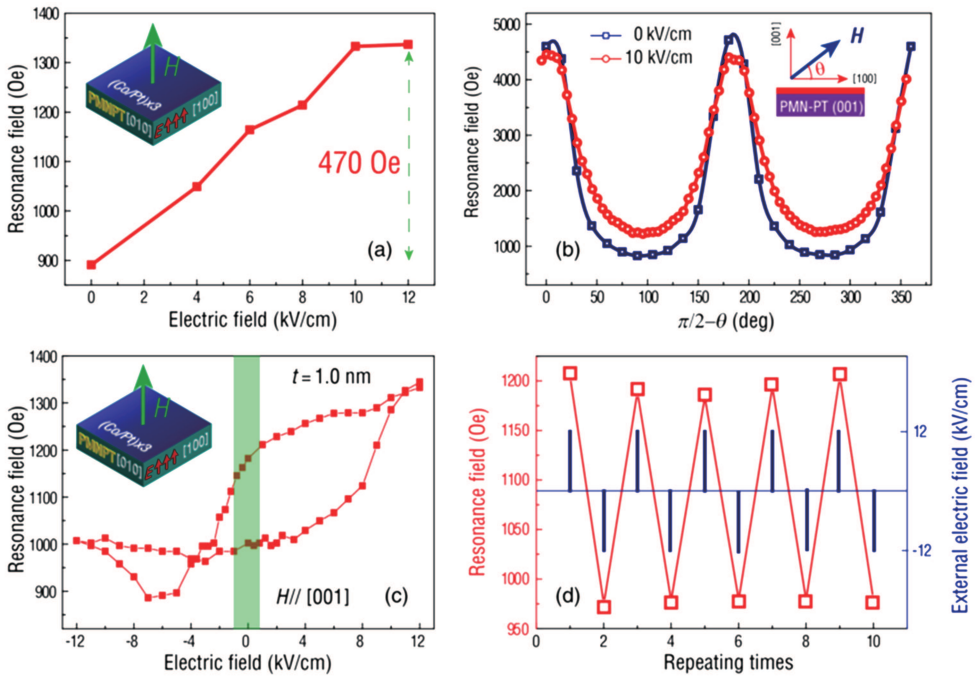


Fig. 3. (color online) The FMR performance of Ta (2 nm)/[Co (1 nm)/Pt (1 nm)]$_3$/Pt (1 nm)/Ta (3 nm)/PMN-PT(001). (a) FMR fields under different applied voltages. (b) Angular dependence of FMR fields at 0 kV/cm and 10 kV/cm. (c) Voltage dependence of FMR fields at the out-of-plane direction. (d) The test results for the repeatability under voltage pulse of $\pm$12 kV/cm.[56]

Yang *et al.* have fabricated Ta (2 nm)/[Co (1 nm)/Pt (1 nm)]$_3$/Pt (1 nm)/Ta (3 nm)/PMN-PT(001) multiferroic multilayers by magnetron sputtering at room temperature to investigate voltage tuning of PMA.[56] The resulting FMR performance is shown in Fig. 3. When an electric field of 12 kV/cm was applied to the heterostructure, a large tunability of 470 Oe

was achieved. To further elucidate the influence of voltage on FMR properties, the angular dependence of the FMR fields was measured for electric fields of 0 kV/cm and 10 kV/cm. The results indicated robust shifts at various angles. Note that the driving voltage suppressed the PMA effect because the difference between the in-plane and out-of-plane anisotropy was observed to decrease. Additionally, two distinct states existed at 0 kV/cm, depending on the different field-sweeping paths (from positive to negative or vice versa). The repeatable and stable modulation of these two distinct statuses has provided a platform to realize nonvolatile information storage. The voltage tuning of PMA might be attributed to the instability of Co orbital moments near the critical transition range. It appeared that the large regulation of FMR fields was due to not only the conventional strain effect, but also to other effects, given that the magnetostriction of the Co/Pt multilayers is relatively small (~ -35 ppm).[52] Thus, the strain-induced lattice strain modulation of the spin reorientation transition (SRT) in the magnetic phase might be a possible reason.[57] Peng *et al.* quantitatively distinguished between the contributions from the common strain effect and the interfacial effect, which is sensitive to lattice strain in Ta (5 nm)/Pt (1 nm)/[Co (1.1 nm)/Pt (1 nm)]$_3$/Ta (3 nm)/PMN-PT(011) at various temperatures.[55]

2.2. Voltage control of FMR via combined effects of strain/stress and other mechanisms

Every mechanism for voltage regulation of magnetism, such as the strain/stress effect, charge effect, exchange coupling effect, electrochemical effect, and orbital reconstruction possess some respective characteristics and common aspects. Sequentially, both cooperation and competition exist among different mechanisms depending on the characteristic thickness of magnetic films.[29] The exploitation of coupling among the different mechanisms to achieve greater modulation of FMR properties might be an efficacious concept.

2.2.1. Strain and charge co-mediated FMR

In the case of magnetoelectric thin films, although the strain/stress-mediated ME coupling is a promising way to achieve large FMR tunability, the substrate clamping effect that has the adverse impacts on the intensity of the ME coupling cannot be negligible. In addition, spin-polarized charge-induced strong ME coupling has been confirmed in a number of multiferroic heterostructures.[28,58–60] Therefore, the combination of these two effects might be an opportunity to enhance ME coupling. The coexistence of strain and charge-induced ME coupling was depicted in Ni/$BaTiO_3$ heterostructures;[61] however, it was generally difficult to distinguish between the contributions of each effect.

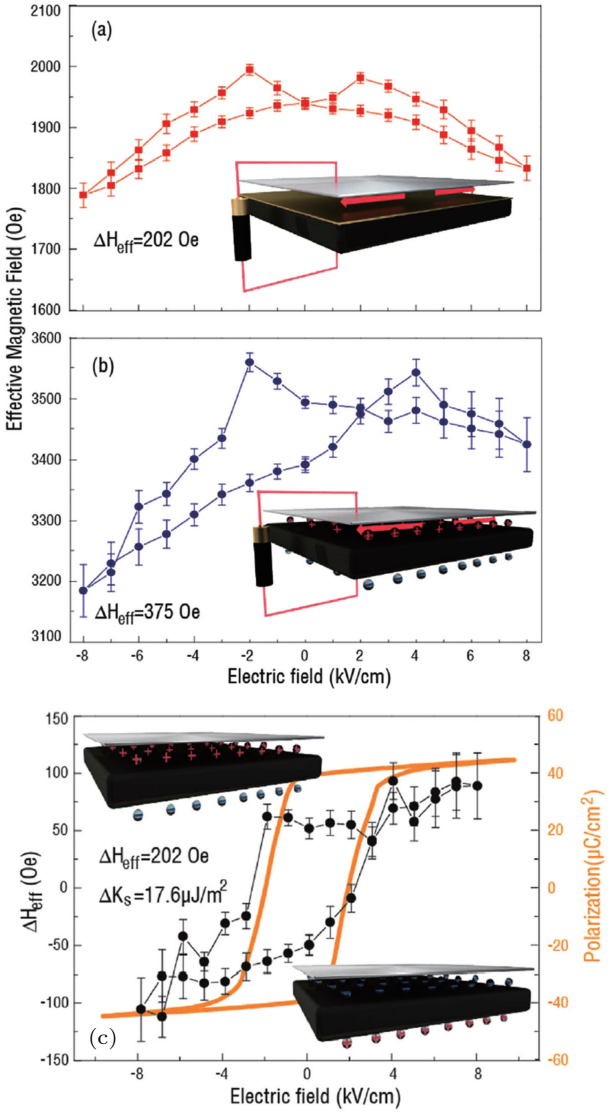


Fig. 4. (color online) FMR fields as a function of the applied voltage in (a) NiFe/Cu/PMN-PT(011) and (b) NiFe/PMN-PT(011) with the magnetic field along the [0$\bar{1}$1] direction. The insets revealed the modification mechanisms in these two aforementioned cases. (c) The pure charge-induced changes of the FMR fields (black) and voltage induced polarization (orange) under different voltages. The inset illustrated the charge accumulation on the NiFe/PMN-PT interface.[62]

Nan *et al.* demonstrated strain and charge co-mediated FMR fields in NiFe/PMN-PT(011) heterostructures and quantitatively distinguished between the contributions from the strain and the charge.[62] Based on the Cu (5 nm)/NiFe (1 nm)/PMN-PT(011) and Cu (5 nm)/NiFe (1 nm)/Cu (5 nm)/PMN-PT(011) multiferroic structures, the FMR field versus voltage were both investigated, and typical results are shown in Fig. 4. In the Cu/NiFe case, the curve of the FMR fields as a function of the applied voltage exhibited obvious asymmetry with a large maximum tunability of 375 Oe. In the case of the Cu/NiFe/Cu heterostructure with Cu as an isolating layer, no screening charge exists at the NiFe/Cu interface. Therefore, the maximum shift of the FMR fields decreased to 202 Oe, and the corresponding H_r-voltage curve formed a standard symmetric butterfly curve. In

other words, a pure strain effect seems to modulate the ME coupling in the Cu/NiFe/Cu/PMN-PT heterostructures. The demonstrated difference between these two switching routes proves the existence of charge-mediated ME coupling. The pure charge-induced tunability was determined to be approximately 202 Oe by calculation. Moreover, the curve of the charge-induced FMR fields as a function of the applied voltage exhibited an analogous shape compared with that of the electrical polarization of PMN-PT.

2.2.2. Strain and surface spin torque co-mediated FMR

Derived from the Landau–Lifshitz–Gilbert equation, the strain-mediated ME coupling could not realize a modification of the damping.[63] Nevertheless, magnetic devices such as memory modules and sensors rely on magnetization switching between equilibrium positions, which inevitably involves a spin relaxation progress of precession that is damping. Thus, voltage manipulation of damping is of considerable importance in the development of high-speed devices.

Jia *et al.* proposed that when a magnetic layer is connected to a ferroelectric layer, a spin-current-carrying surface magnetic order is excited on the scale of the spin diffusion length.[64] The induced spin torque could be utilized to achieve voltage tuning of the magnetism. Subsequently, this concept was further confirmed by experiments in CoZr/PMN-PT.[63] Jia *et al.* deposited CoZr (20 nm) films on PMN-PT(011) substrates using RF magnetron sputtering. Simultaneously, CoZr (20 nm)/Ta (5 nm)/PMN-PT(011) multilayers were fabricated under the same condition. Figure 5(a) reveals FMR plots under different applied voltages and indicates distinct changes in the FMR fields and FMR linewidths. The asymmetric resonance lineshape might be attributed to the mixture of the imaginary and real part of the susceptibility.[65] To quantitatively determine the tunability due to voltage adjustment, the acquired experimental data were integrated and then fitted to an asymmetric Lorentzian lineshape. The FMR fields (H_r) and effective linewidth (Δ_{eff}, $\Delta_{\text{eff}} = \Delta \cos \omega$, Δ is the half-maximum linewidth and ω represents the mixture phase between the real and imaginary part of the susceptibility) are shown in Fig. 5(b). An increasingly negative surface spin density derived from the approximately linear dependence between the FMR fields versus the applied voltage caused the diminution of the damping and the effective linewidth. For comparison, the FMR properties were measured in CoZr/Ta/PMN-PT multilayers by using the same experimental steps, as shown in Fig. 5(c). Clearly, the tunability of the FMR linewidth was absent in the presence of only the strain effect.

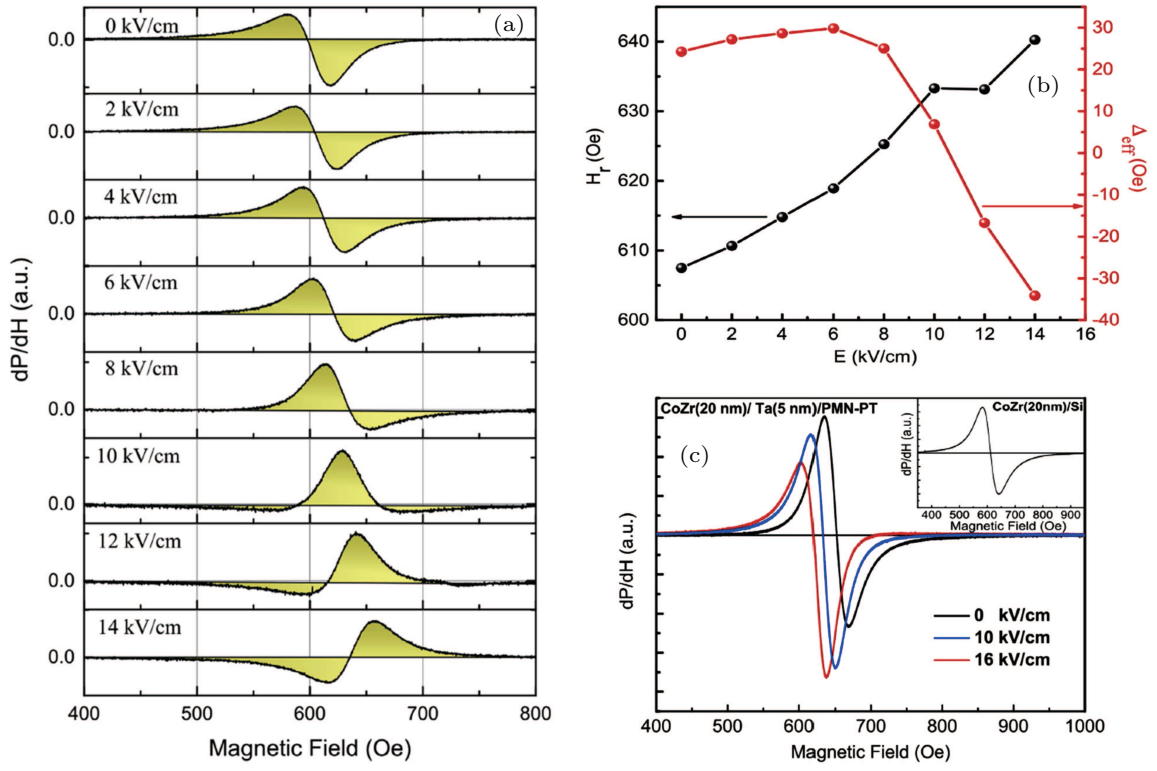


Fig. 5. (color online) (a) The FMR spectra and (b) tunability of FMR fields and the effective linewidth of CoZr (20 nm)/PMN-PT(011) heterostructures under various applied voltages at a fixed frequency of 8.969 GHz. (c) The FMR spectra of CoZr (20 nm)/Ta (5 nm)/PMN-PT(011) multilayers at different applied voltages. The inset represents a symmetric spectrum of the CoZr/Si structures.[63]

2.3. Voltage control of FMR via ionic liquid gating

Ionic liquid possesses wide electrochemical stability windows, high ionic conductivity at ambient conditions, low vapor pressure, and chemical flexibility.[66–68] When a voltage is applied, two kinds of ions with opposite polarity separate from each other in the ionic liquid and automatically move towards the cathode and anode. Accordingly, the charges which accumulate on one side of the ionic liquid/sample interface induce opposite charges on the other side to form an electric double layer (EDL). The high charge density in the EDL could change the physical properties of the interfacial layer. Compared with the strain/stress method, voltage tuning of magnetism utilizing ionic liquid gating could further decrease the required voltage of the circuit voltage (< 5 V) and has good compatibility with various substrates.[29] So far, it has been reported that insulator-to-metal transition, transport performance of the p–n junction, and magnetic anisotropy can be manipulated via ionic liquid gating.[69–73] It is worth noting that Yang *et al.* realized the transition between antiferromagnetic and ferromagnetic ordering in synthetic antiferromagnetic films through voltage regulation of Ruderman–Kittel–Kasuya–Yosida (RKKY) interactions induced by utilizing ionic liquid gating.[74] Nevertheless, the intrinsic mechanism of ionic liquid modulation is still being debated.

Recently, Zhao *et al.* demonstrated voltage control of FMR fields via ionic liquid gating in Au/$[DEME]^+$ $[TFSI]^-$/Co (2.25 nm) heterostructures.[75] In this case, two regions were considered, an electrostatic doping region (region I, $-1.3\ \text{V} < V_g < +2.3\ \text{V}$) and an electrochemical reaction region (region II, $V_g \leq -1.3$ V or $V_g \geq +2.3$ V). The experimental results of ionic liquid gating of FMR fields in region I are shown in Fig. 6, in which electrostatic doping dominated the voltage regulation of the magnetism. The angular dependence of the FMR fields indicated that a tunability of 219 Oe was realized at 70 ° at 1.5 V, corresponding to a giant ME coefficient of 146 Oe/V. The FMR properties under different applied voltages could be clearly depicted with the aid of a contour map. Figure 6(c) indicates that a giant FMR field shift could be achieved under a positive voltage; however, negative voltage had little effect on the FMR fields. More importantly, ionic liquid gating could facilitate reversible manipulation of the FMR fields. In region II, a large FMR tunability of 415 Oe was achieved at 70 ° under 5 V without reversibility. In this case, the main reason for voltage modulation was due to an electrochemical reaction. Therefore, ionic liquid gating has demonstrated the potential to change the FMR field with circuit-operating voltages (< 5 V). However, more work is needed to improve the operating speed as the current working time of ionic liquid gating is typically more than 1 min.

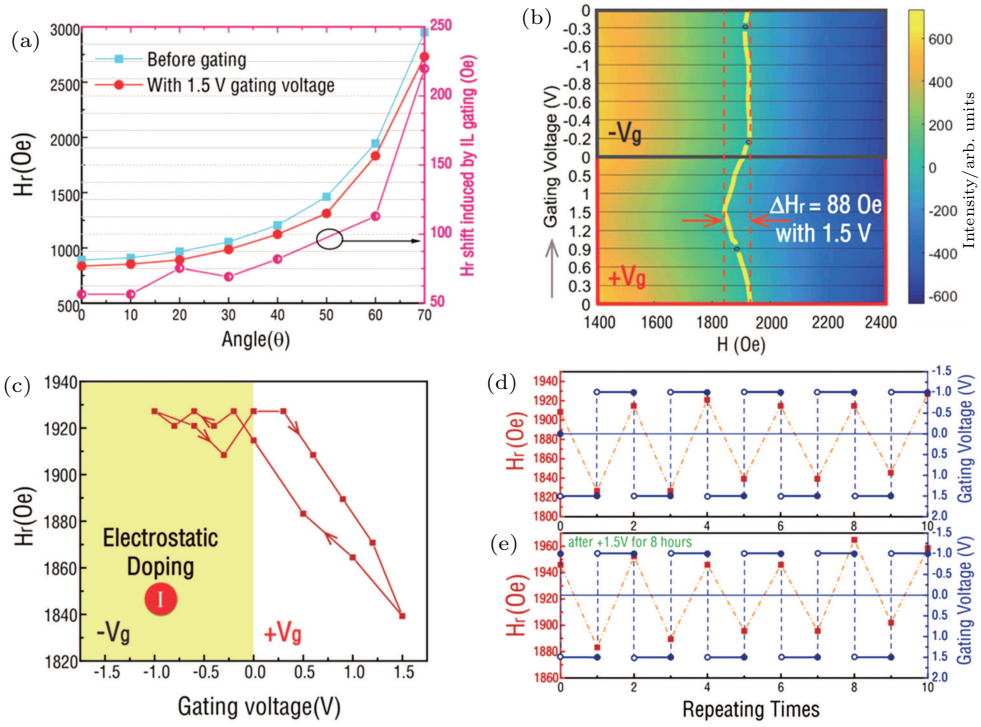


Fig. 6. (color online) Ionic liquid gating of FMR fields with electrostatic doping dominating the regulation of the magnetism. (a) Angular dependence of the FMR fields. The blue line represents the initial state, the red line represents the state with a 1.5 V gating voltage, and the pink line represents the shift of the FMR fields. 0° indicates the in-plane direction. (b) The FMR phase diagram. The yellow line represents the FMR fields under different applied voltages at 60°. (c) The FMR fields under different applied voltages at 60°. (d) and (c) Reproducible measurements and the same tests after applying +1.5 V for 8 h.[75]

3. Voltage tuning of spin waves

As mentioned above, owing to the fact that spin waves have distinct advantages such as a wide frequency range (GHz to THz), immunity to Joule heat dissipation, and a wide physical toolbox, spin-wave-based devices have promising prospects for practical applications.[7,8] The modification of spin wave related behavior has been achieved with the help of shape anisotropy, magnetic domain walls, spin current, voltage, etc.[76–79] Moreover, voltage regulation appears to be an energy efficient way to regulate spin waves.

3.1. Voltage control of spin waves

According to Eq. (1), spin waves can be modulated by changing the interfacial conditions. Zhu *et al.* reported the control of spin waves in $La_{0.5}Sr_{0.5}MnO_3$(LSMO5)/PMN-PT(001) heterostructures, utilizing the voltage induced strain/stress effects.[80] An applied electric field of 20 kV/cm shifted the angle at which the spin waves vanished from 67° to 71° with a tunability of 4°. The response of spin waves to the applied voltage varied with angles, as shown in Fig. 7. At 60°, no peaks from surface spin waves could be detected. At 80°, higher order spin waves were present at the applied voltage. Furthermore, from the out-of-plane direction, the SWR was changed by 187 Oe while the FMR tunability was 169 Oe. The voltage modulation of the surface spin waves was attributed to lattice deformation of magnetic films caused by the voltage induced stress/strain.

Voltage control of the spin waves can be achieved not only in ferrite/piezoelectric heterostructures, but also in metal/piezoelectric composites. Ziętek *et al.* presented results for voltage manipulation of standing spin waves resonance (SSWR) in patterned NiFe (20 nm)/PMN-PT(011) microstrips with a shift of 22 Oe under 2 kV/cm at 5 GHz.[81] Standing spin waves (SSW) are formed by the interference between waves reflected back and forth. Furthermore, Cazayous *et al.* also realized voltage control of spin waves frequency in single-phase multiferroic $BiFeO_3$ with a tunability of over 30%.[82] Non-volatile regulation and extremely low power consumption make $BiFeO_3$ one of the promising candidates for spin-wave-based device applications.

A better choice for spin-wave-based device development is to utilize an applied voltage to generate spin waves, which would further reduce the overall power consumption.[83] Cherepov *et al.* proposed and confirmed voltage excitation of spin waves in multiferroic magnetoelectric (ME) cells, as shown in Figs. 8(a) and 8(b).[83] The alternating voltage applied to the PMN-PT slab generated an oscillating strain in the piezoelectric phase, which was transferred to the magnetic spin wave bus that stimulated the spin waves. Figure 8(c) shows the reflection signals (S_{22}) from the ME cell, thereby demonstrating magnetization excitation using an applied voltage. In addition, the transmission signal (S_{12}) between two identical ME cells indicated that spin waves could be generated and detected using ME cells, as shown in Fig. 8(d). This research has demonstrated that voltage control of spin waves is promising for device applications.

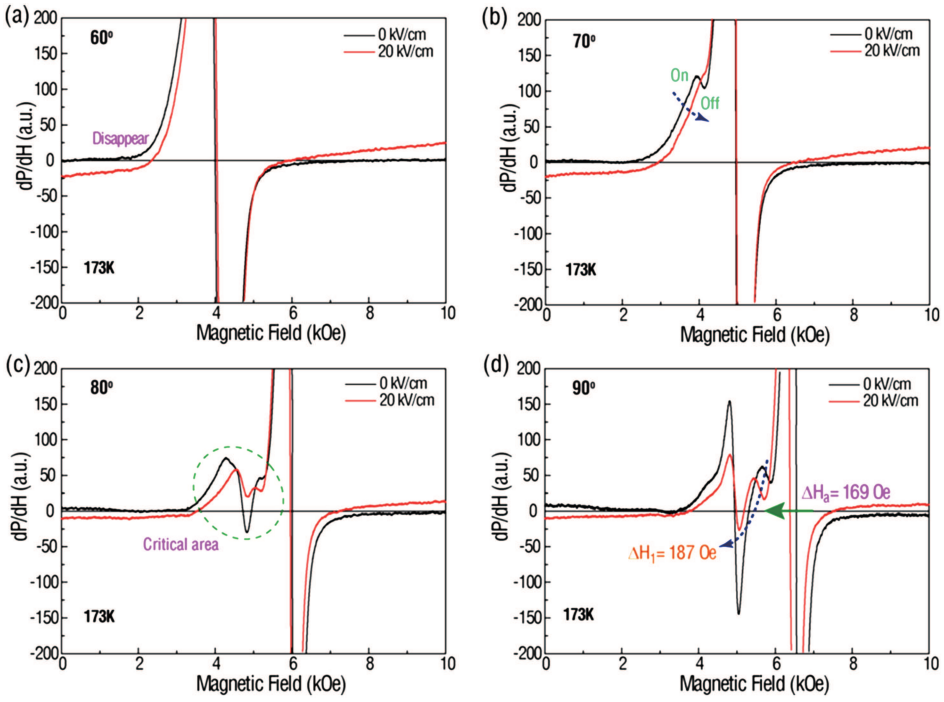


Fig. 7. (color online) Angular dependence of spin wave behaviors obtained in LSMO5/PMN-PT multiferroic heterostructures at 173 K at various applied voltages when the H-fields angles were (a) 60°, (b) 70°, (c) 80°, and (d) 90°, respectively. Arrows indicate the variation trend of the SWR spectra relative to the applied voltage.[80]

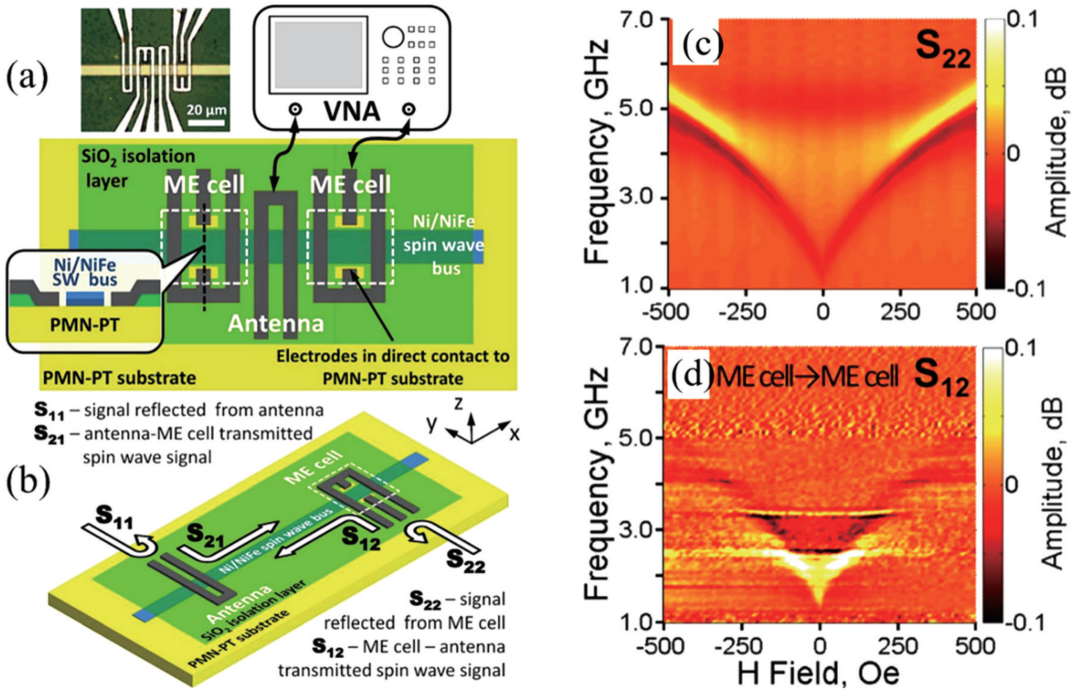


Fig. 8. (color online) (a) Schematic of the investigated device and the performed measurements via a vector network analyzer. The PMN-PT(110) was partially covered by SiO_2 isolation, with dedicated openings in the SiO_2 layer to directly attach the electrodes of the ME cell. The spin wave bus was a 5 μm wide Ni (20 nm)/NiFe (20 nm) bilayer. Aluminum loop antennas having a thickness of 200 nm and ME cells were designed for spin wave excitation and detection. (b) Schematic of the setup for two-port measurements of reflection and transmission signals. The experimental results of (c) reflection signals from ME cell and (d) the transmission signals between two identical ME cells, respectively.[83]

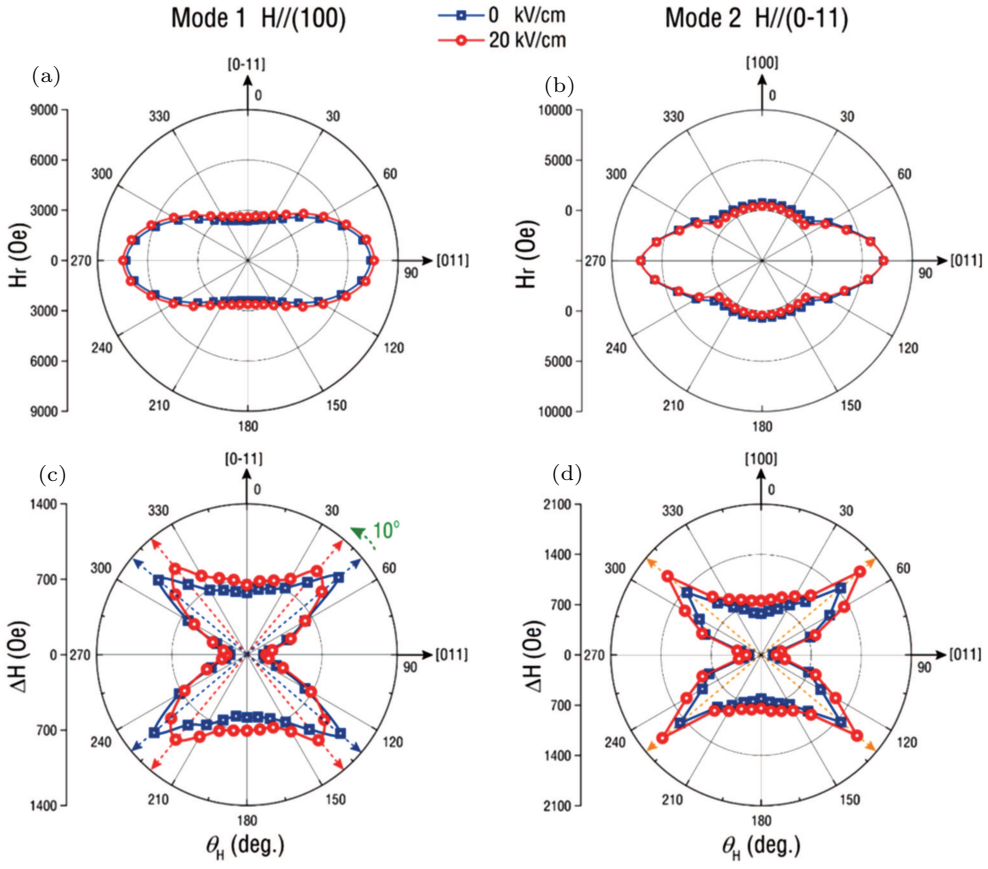


Fig. 9. (color online) Angular dependence of voltage regulation of (a), (b) FMR fields and (c), (d) linewidths of NZFO/PMN-PT(011) heterostructures in mode 1 (the magnetic field is within the (100) plane of PMN-PT) and in mode 2 (the magnetic field is within the (011) plane of PMN-PT), respectively. The critical angles are marked with arrows.[91]

3.2. Two-magnon scattering related spin waves

Voltage control of spin dynamics is attractive because of the related rich physical phenomena and the great potential with regard to spintronic devices. The two-magnon scattering (TMS) effect involves the transfer of microwave energy to the degenerate spin wave with the same precession frequency and nonzero wave vector.[84–89] In brief, it is an extrinsic magnetic loss mechanism dominated by spin waves. Therefore, from the perspective of applications, it is significant to modulate the TMS effect using an applied voltage. The TMS effect is usually manifested as FMR fields changing or linewidth broadening[84,86] and widely exists in various ferromagnets.[85–87,90] Xue *et al.* confirmed the voltage tuning of TMS in $Ni_{0.5}Zn_{0.5}Fe_2O_4$ (NZFO)/ PMN-PT(011) multiferroic heterostructures fabricated by PLD.[91] Owing to the in-plane anisotropy of the PMN-PT(011) slabs, the voltage modification of the TMS was divided into two modes as the magnetic field was parallel to the (100) or $(0\bar{1}1)$ plane of the PMN-PT substrates, respectively. The voltage control of TMS under different voltages for these two modes was depicted in Figs. 9(a) and 9(b). It is noteworthy that in the case of mode 2, the applied voltage induced an easy axis rotation from the in-plane direction to the TMS critical angle. The voltage regulation of the FMR linewidth at TMS critical angles exhibited the opposite trend in the aforementioned two modes with a tunability of 23.15% at 300 K, as shown in Figs. 9(c) and 9(d). The compressive strain in mode 1 resulted in a reduction of the linewidth while the tensile strain in mode 2 led to an increase in the linewidth. It is particularly noteworthy that the strongest spin-wave damping angle shifted from 50° to 40° under an applied electric field of 20 kV/cm. The voltage modification of the TMS was also observed in $La_{0.7}Sr_{0.3}MnO_3$ (LSMO)/PMN-PT(011) multiferroic heterostructure, thus highlighting another method to control spin waves indirectly.[92]

4. Prospects

In recent years, there has been considerable interest on voltage manipulation of FMR and SWR in ME composites. Studies on FMR provide a quantitative way to characterize the spatial distribution of magnetic anisotropy, and the voltage control method makes magnetism regulation more energy-efficient. These observations are of great significance in potential applications of ultra-high frequency microwave devices. However, there are still some problems that need to be solved. Most of the current studies are focused on strain-mediated ME couplings based on thin magnetic films deposited on thick piezoelectric substrates, where the substrate clamping effects have adverse impacts on the intensity of the ME coupling. Furthermore, the working voltage to modulate magnetism needs to be further reduced. With respect to the progress made in ionic liquid gating, the response time is a major concern as well as the potential for liquid leakage and pollution problems. Releasing films from substrates is a promising way to overcome these challenges, especially for those devices that are based on strain-related mechanisms. It is also necessary to develop ME coupling in nanocomposites in detail. Self-assembly techniques should also be explored to enhance the ME response in such systems.

The most important limitations for the practical use of voltage control of FMR and SWR include the following. (i) The physical mechanism needs to be clarified, especially for those samples with two or more coupling mechanisms. (ii) New material systems with narrow FMR linewidths and low magnetic damping are required for RF/microwave applications. (iii) Existing control methods such as the strain-mediated and ionic liquid gating still have their limitations; hence, novel control methods with high speeds and low circuit voltages need to be explored. Thus, the full potential of voltage-tunable FMR and SWR is yet to be realized.

References

[1] Owens J M, Collins J H and Carter R L 1985 *Circuits Syst. Signal Process.* **4** 317
[2] Adam J D 1988 *Proc. IEEE* **76** 159
[3] Sato N, Sekiguchi K and Nozaki Y 2013 *Appl. Phys. Express* **6** 063001
[4] Khitun A and Wang K L 2011 *J. Appl. Phys.* **110** 034306
[5] Balashov T, Buczek P, Sandratskii L, Ernst A and Wulfhekel W 2014 *J. Phys.: Condens. Matter* **26** 394007
[6] Cherepanov V, Kolokolov I and Lvov V 1993 *Phys. Rep.* **229** 81
[7] Chumak A V, Serga A A and Hillebrands B 2014 *Nat. Commun.* **5** 4700
[8] Chumak A V, Vasyuchka V I, Serga A A and Hillebrands B 2015 *Nat. Phys.* **11** 453
[9] Farle M 1998 *Rep. Prog. Phys.* **61** 755
[10] Aleshkevych P, Baran M, Dyakonov V, Szymczak R, Szymczak H, Baberschke K, Lindner J and Lenz K 2006 *Phys. Stat. Sol. (a)* **203** 1586
[11] Puszkarski H 1970 *Acta Phys. Pol. A* **A38** 217
[12] Puszkarski H 1972 *Phys. Status Solidi* **50** 87
[13] Ikeda S, Miura K, Yamamoto H, Mizunuma K, Gan H D, Endo M, Kanai S, Hayakawa J, Matsukura F and Ohno H 2010 *Nat. Mater.* **9** 721
[14] Sato H, Yamamoto T, Yamanouchi M, Ikeda S, Fukami S, Kinoshita K, Matsukura F, Kasai N and Ohno H 2013 *Tech. Dig. Int. Electron Devices Meeting*, December, Washington DC, USA p. 60
[15] Shiota Y, Nozaki T, Bonell F, Murakami S, Shinjo T and Suzuki Y 2012 *Nat. Mater.* **11** 39
[16] Zhang N, Zhang B, Yang M Y, Cai K M, Sheng Y, Li Y C, Deng Y C and Wang K Y 2017 *Acta Phys. Sin.* **66** 027501 (in Chinese)
[17] Matsukura F, Tokura Y and Ohno H 2015 *Nat. Nanotech.* **10** 209
[18] Wang W G, Li M, Hageman S and Chien C L 2012 *Nat. Mater.* **11** 64
[19] Cai K, Yang M, Ju H, Wang S, Ji Y, Li B, Edmonds K W, Sheng Y, Zhang B, Zhang N, Liu S, Zheng H and Wang K 2017 *Nat. Mater.* **16** 712
[20] Zhang B, Meng K K, Yang M Y, Edmonds K W, Zhang H, Cai K M, Sheng Y, Zhang N, Ji Y, Zhao J H, Zheng H Z and Wang K Y 2016 *Sci. Rep.* **6** 28458
[21] Jian-Xin S, Da-Shan S and Young S 2018 *Acta Phys. Sin.* **67** 127501 (in Chinese)
[22] Lou J, Liu M, Reed D, Ren Y and Sun N X 2009 *Adv. Mater.* **21** 4711
[23] He H, Zhao J T, Luo Z L, Yang Y J, Xu H, Hong B, Wang L X, Wang R X and Gao C 2016 *Chin. Phys. Lett.* **33** 067502
[24] Li Q, Wang D H, Cao Q Q and Du Y W 2017 *Chin. Phys. B* **26** 097502
[25] Duan C G, Velev J P, Sabirianov R F, Zhu Z, Chu J, Jaswal S S and Tsymbal E Y 2008 *Phys. Rev. Lett.* **101** 137201

[26] Heron J T, Bosse J L, He Q, Gao Y, Trassin M, Ye L, Clarkson J D, Wang C, Liu J, Salahuddin S, Ralph D C, Schlom D G, Iniguez J, Huey B D and Ramesh R 2014 *Nature* **516** 370

[27] Li H B, Lu N, Zhang Q, Wang Y, Feng D, Chen T, Yang S, Duan Z, Li Z, Shi Y, Wang W, Wang W H, Jin K, Liu H, Ma J, Gu L, Nan C and Yu P 2017 *Nat. Commun.* **8** 2156

[28] Maruyama T, Shiota Y, Nozaki T, Ohta K, Toda N, Mizuguchi M, Tulapurkar A A, Shinjo T, Shiraishi M, Mizukami S, Ando Y and Suzuki Y 2009 *Nat. Nanotech.* **4** 158

[29] Song C, Cui B, Li F, Zhou X and Pan F 2017 *Prog. Mater. Sci.* **87** 33

[30] Hu J M, Chen L Q and Nan C W 2016 *Adv. Mater.* **28** 15

[31] Song C, Cui B, Peng J, Mao H and Pan F 2016 *Chin. Phys. B* **25** 067502

[32] Barnes S E 1981 *Adv. Phys.* **30** 801

[33] Heinrich B and Cochran J F 1993 *Adv. Phys.* **42** 523

[34] Liu X Y and Furdyna J K 2006 *J. Phys.: Condens. Matter* **18** R245

[35] Zhou Z, Peng B, Zhu M and Liu M 2016 *J. Adv. Dielect.* **06** 1630005

[36] Gu W J, Pan J and Hu J G 2012 *Acta Phys. Sin.* **61** 167501 (in Chinese)

[37] Liu M, Howe B M, Grazulis L, Mahalingam K, Nan T, Sun N X and Brown G J 2013 *Adv. Mater.* **25** 4886

[38] Liu M, Obi O, Lou J, Chen Y, Cai Z, Stoute S, Espanol M, Lew M, Situ X, Ziemer K S, Harris V G and Sun N X 2009 *Adv. Funct. Mater.* **19** 1826

[39] Hu Z, Wang X, Nan T, *et al.* 2016 *Sci. Rep.* **6** 32408

[40] Sun Y, Ba Y, Chen A, *et al*, 2017 *ACS Appl. Mater. Interfaces* **9** 10855

[41] Shi Z P, Liu X M and Li S D 2017 *Chin. Phys. B* **26** 097601

[42] Liu M, Obi O, Cai Z, Lou J, Yang G, Ziemer K S and Sun N X 2010 *J. Appl. Phys.* **107** 073916

[43] Nozaki T, Shiota Y, Miwa S, Murakami S, Bonell F, Ishibashi S, Kubota H, Yakushiji K, Saruya T, Fukushima A, Yuasa S, Shinjo T and Suzuki Y 2012 *Nat. Phys.* **8** 491

[44] Liu M, Li S, Zhou Z, Beguhn S, Lou J, Xu F, Jian Lu T and Sun N X 2012 *J. Appl. Phys.* **112** 603917

[45] Ignatchenko V A and Felk V A 2005 *Phys. Rev. B* **71** 094417

[46] Liu M, Zhou Z, Nan T, Howe B M, Brown G J and Sun N X 2013 *Adv. Mater.* **25** 1435

[47] Xing X, Liu M, Li S D, Obi O, Lou J, Zhou Z, Chen B and Sun N X 2011 *IEEE Trans. Magn.* **47** 3104

[48] Yang X, Liu M, Peng B, Zhou Z Y, Nan T X, Sun H J and Sun N X 2015 *Appl. Phys. Lett.* **107** 122408

[49] Yuan G, Zare S, Onabajo M, Ming L, Ziyao Z, Tianxiang N, Xi Y, Ming L, Mahalingam K, Howe B M, Jones J G, Brown G J and Sun N X 2014 2014 *IEEE MTT-S International Microwave Symposium (IMS2014)* 1–6 June, 2014 p. 4

[50] Gao Y, Wang X, Xie L, Hu Z, Lin H, Zhou Z, Nan T, Yang X, Howe B M, Jones J G, Brown G J and Sun N X 2016 *Appl. Phys. Lett.* **108** 232903

[51] Chen X, Liu H F, Han X F and Ji Y 2013 *Acta Phys. Sin.* **62** 137501 (in Chinese)

[52] Shepley P M, Rushforth A W, Wang M, Burnell G and Moore T A 2015 *Sci. Rep.* **5** 7921

[53] Kim J H, Ryu K S, Jeong J W and Shin S C 2010 *Appl. Phys. Lett.* **97** 252508

[54] Lei N, Park S, Lecoeur P, Ravelosona D, Chappert C, Stelmakhovych O and Holý V 2011 *Phys. Rev. B* **84** 012404

[55] Peng B, Zhou Z, Nan T, Dong G, Feng M, Yang Q, Wang X, Zhao S, Xian D, Jiang Z D, Ren W, Ye Z G, Sun N X and Liu M 2017 *ACS Nano* **11** 4337

[56] Yang Q, Nan T, Zhang Y, Zhou Z, Peng B, Ren W, Ye Z G, Sun N X and Liu M 2017 *Phys. Rev. Appl.* **8** 044006

[57] Pertsev N A 2008 *Phys. Rev. B* **78** 212102

[58] Molegraaf H J A, Hoffman J, Vaz C A F, Gariglio S, van der Marel D, Ahn C H and Triscone J M 2009 *Adv. Mater.* **21** 3470

[59] Endo M, Kanai S, Ikeda S, Matsukura F and Ohno H 2010 *Appl. Phys. Lett.* **96** 212503

[60] Shiota Y, Murakami S, Bonell F, Nozaki T, Shinjo T and Suzuki Y 2011 *Appl. Phys. Exp.* **4** 043005

[61] Shu L, Li Z, Ma J, Gao Y, Gu L, Shen Y, Lin Y and Nan C W 2012 *Appl. Phys. Lett.* **100** 022405

[62] Nan T, Zhou Z, Liu M, *et al.* 2015 *Sci. Rep.* **4** 3688

[63] Jia C, Wang F, Jiang C, Berakdar J and Xue D 2015 *Sci. Rep.* **5** 11111

[64] Jia C L, Wei T L, Jiang C J, Xue D S, Sukhov A and Berakdar J 2014 *Phys. Rev. B* **90** 054423

[65] Hoffmann F, Woltersdorf G, Wegscheider W, Einwanger A, Weiss D and Back C H 2009 *Phys. Rev. B* **80** 054417

[66] Galiński M, Lewandowski A and Stępniak I 2006 *Electrochim. Acta* **51** 5567

[67] Arm M, Endres F, MacFarlane D R, Ohno H and Scrosati B 2009 *Nat. Mater.* **8** 621

[68] Lodge T P 2008 *Science* **321** 50

[69] Yi H T, Gao B, Xie W, Cheong S W and Podzorov V 2015 *Sci. Rep.* **4** 6604

[70] Shi W, Ye J, Checkelsky J G, Terakura C and Iwasa Y 2014 *Adv. Funct. Mater.* **24** 2005

[71] Zhang Y J, Ye J T, Yomogida Y, Takenobu T and Iwasa Y 2013 *Nano Lett.* **13** 3023

[72] Cui B, Song C, Wang G Y, Yan Y N, Peng J J, Miao J H, Mao H J, Li F, Chen C, Zeng F and Pan F 2014 *Adv. Funct. Mater.* **24** 7233

[73] Cui B, Song C, Gehring G A, Li F, Wang G Y, Chen C, Peng J J, Mao H J, Zeng F and Pan F 2015 *Adv. Funct. Mater.* **25** 864

[74] Yang Q, Wang L, Zhou Z, Wang L, Zhang Y, Zhao S, Dong G, Cheng Y, Min T, Hu Z, Chen W, Xia K and Liu M 2018 *Nat. Commun.* **9** 991

[75] Zhao S, Zhou Z, Peng B, Zhu M, Feng M, Yang Q, Yan Y, Ren W, Ye Z G, Liu Y and Liu M 2017 *Adv. Mater.* **29** 1606478

[76] Haldar A, Kumar D and Adeyeye A O 2016 *Nat. Nanotech.* **11** 437

[77] Wagner K, Kakay A, Schultheiss K, Henschke A, Sebastian T and Schultheiss H 2016 *Nat. Nanotech.* **11** 432

[78] Demidov V E, Urazhdin S, Ulrichs H, Tiberkevich V, Slavin A, Baither D, Schmitz G and Demokritov S O 2012 *Nat. Mater.* **11** 1028

[79] Zhu M, Zhou Z, Peng B, Zhao S, Zhang Y, Niu G, Ren W, Ye Z G, Liu Y and Liu M 2017 *Adv. Funct. Mater.* **27** 1605598

[80] Zhu M, Zhou Z, Xue X, Guan M, Xian D, Wang C, Hu Z, Jiang Z D, Ye Z G, Ren W and Liu M 2017 *Appl. Phys. Lett.* **111** 102903

[81] Ziętek S, Chęciński J, Frankowski M, Skowroński W and Stobiecki T 2017 *J. Magn. Magn. Mater.* **428** 64

[82] Rovillain P, de Sousa R, Gallais Y, Sacuto A, Measson M A, Colson D, Forget A, Bibes M, Barthelemy A and Cazayous M 2010 *Nat. Mater.* **9** 975

[83] Cherepov S, Khalili Amiri P, Alzate J G, Wong K, Lewis M, Upadhyaya P, Nath J, Bao M, Bur A, Wu T, Carman G P, Khitun A and Wang K L 2014 *Appl. Phys. Lett.* **104** 082403

[84] Arias R and Mills D L 1999 *Phys. Rev. B* **60** 7395

[85] Srivastava A K, Hurben M J, Wittenauer M A, Kabos P, Patton C E, Ramesh R, Dorsey P C and Chrisey D B 1999 *J. Appl. Phys.* **85** 7838

[86] Azevedo A, Oliveira A B, de Aguiar F M and Rezende S M 2000 *Phys. Rev. B* **62** 5331

[87] Zakeri K, Lindner J, Barsukov I, Meckenstock R, Farle M, von Hörsten U, Wende H, Keune W, Rocker J, Kalarickal S S, Lenz K, Kuch W, Baberschke K and Frait Z 2007 *Phys. Rev. B* **76** 104416

[88] Landeros P, Arias R E and Mills D L 2008 *Phys. Rev. B* **77** 214405

[89] Lindner J, Barsukov I, Raeder C, Hassel C, Posth O, Meckenstock R, Landeros P and Mills D L 2009 *Phys. Rev. B* **80** 224421

[90] Qiao S Z, Ren Q N, Hao R R, Zhong H, Kang Y, Kang S S, Qin Y F, Yu S Y, Han G B, Yan S S and Mei L M 2016 *Chin. Phys. Lett.* **33** 047601

[91] Xue X, Dong G, Zhou Z, Xian D, Hu Z, Ren W, Ye Z G, Chen W, Jiang Z D and Liu M 2017 *ACS Appl. Mater. Interfaces* **9** 43188

[92] Xue X, Zhou Z, Dong G, Feng M, Zhang Y, Zhao S, Hu Z, Ren W, Ye Z G, Liu Y and Liu M 2017 *ACS Nano* **11** 9286